OPEN

Citation: Cell Death and Disease (2014) 5, e1175; doi:10.1038/cddis.2014.144

www.nature.com/cddis

Impaired mitochondrial respiration promotes dendritic branching via the AMPK signaling pathway

A Gioran[1], P Nicotera[1] and D Bano*,[1]

Functional neuronal circuits require a constant remodeling of their network composed of highly interconnected neurons. The plasticity of synapses and the shaping of elaborated dendritic branches are energy demanding and therefore depend on an efficient mitochondrial oxidative phosphorylation (OXPHOS). The spatial and functional regulations of dendritic patterning occur also after cell fate specification; however, the molecular mechanisms underlying this complex process remain elusive. Here, we exploit the changes in dendritic architecture in highly branched neurons as a result of aberrant mitochondrial activity. In sensory neurons of *Caenorhabditis elegans*, genetic manipulations of mitochondrial complex I subunits cause an unexpected outgrowth of dendritic arbors and ectopic structures. The increased number of dendritic branches is coordinated through a specific signaling cascade rather than as a simple consequence of oxidative stress. On the basis of genetic and pharmacological evidence, we show that OXPHOS deficiency promotes branching through the activation of the AMP-activated protein kinase AMPK and the downstream target phosphoinositide 3-kinase PI3K. Taken together, our findings describe a well-defined signaling pathway that regulates dendritic outgrowth in conditions of compromised OXPHOS and the resulting AMPK activation.
Cell Death and Disease (2014) **5,** e1175; doi:10.1038/cddis.2014.144; published online 10 April 2014
Subject Category: Neuroscience

Mitochondria are intracellular double-membrane organelles that take part in a wide range of cellular processes, including nutrient catabolism, biosynthesis of metabolic intermediates, signaling and energy production via oxidative phosphorylation (OXPHOS). The OXPHOS system comprises the respiratory chain and the ATP synthase that generates ATP from ADP and inorganic phosphate. In the cytosol and in the mitochondrial matrix, the oxidation of fuel substrates from different carbon sources generates NADH and $FADH_2$. These reduced molecules provide equivalents to the electron transport chain (ETC), consisting of four multisubunit complexes embedded in the mitochondrial inner membrane and two mobile electron carriers.[1,2] Based on recent evidence, the electron flux occurs in quaternary supramolecular structures, also called respirasomes, rather than as a result of random encounters between individual ETC components.[3,4] The transport of electrons to molecular oxygen as the final acceptor is coupled with the formation of a proton gradient across the membrane. This membrane potential is then dissipated by the complex V/ATP synthases for energy production or for the maintenance of other metabolic activities. Mitochondria retain evident vestiges of their original endosymbiotic prokaryotic ancestor. Apart from the highly dynamic double membrane, mitochondria contain a circular genome that encodes genes involved in mitochondrial protein translation and 13 essential subunits of the complex I, III, IV and V of the OXPHOS system. The remaining thousand or so proteins are nuclear encoded and actively imported in the mitochondria, where they need to be assembled into functionally organized complexes.[5]

Given their essential role in cellular metabolism, genetically inherited mutations as well as off-target effects of chemical compounds that disturb mitochondrial functions can seriously impinge healthy lifespan and inevitably lead to severe syndromes or progressive degenerative pathologies.[2,6–8] From the clinical standpoint, human diseases caused by mitochondrial impairment exhibit heterogeneous manifestations that range from single tissue lesions to multiple organ failure. The vulnerability of cell types, the evoked clinical aspect and the age of onset of the disease depend on the extent of the mitochondrial damage. In eukaryotic cells, adaptive stress-responsive pathways partially respond to mitochondrial defects by promoting defensive mechanisms and alternative routes of energy production that, at least in some animal models, can ultimately result in lifespan extension.[8,9] However, when the cellular damage exceeds a certain threshold, these compensatory processes are not sufficient to prevent deleterious effects on cellular maintenance, thus resulting in various diseases. As a quantitative decline of mitochondrial activity occurs during aging, faulty OXPHOS contributes to the onset of age-related human pathologies, including many common neurodegenerative diseases such as Parkinson's and Alzheimer's disease. The discovery that several inherited forms of brain disorders are due to mutations in genes involved in mitochondrial activity supports this view.[10] Yet, how OXPHOS impairment can affect neuronal activity, neural branching and the plasticity of neural circuits remains an important open question. Therefore, the use of animal models carrying OXPHOS defects represents a useful tool for dissecting

[1]German Center for Neurodegenerative Diseases (DZNE), Bonn, Germany
*Corresponding author: D Bano, Deutsches Zentrum für Neurodegenerative Erkrankungen (DZNE), Ludwig-Erhard-Allee 2, D-53175 Bonn, Germany. Tel: +49 228 43302510; Fax: +49 228 43302689; E-mail: daniele.bano@dzne.de
Keywords: AMPK; *Caenorhabditis elegans*; dendritic branching; mitochondria; OXPHOS
Abbreviations: AICAR, 5-aminoimidazole-4-carboxamide ribonucleotide; AMPK, 5′-adenosine monophosphate-activated protein kinase; *C. elegans*, *Caenorhabditis elegans*; OXPHOS, oxidative phosphorylation; PI3K, phosphatidylinositol-4,5-bisphosphate 3-kinase
Received 14.2.14; accepted 27.2.14; Edited by A Verkhratsky

in vivo signaling cascades with therapeutic relevance not only for inherited 'mitochondrial disorders' but also for many other human brain pathologies.[5]

The nematode *Caenorhabditis elegans* is a transparent free-living organism with highly characterized embryonic and larval development. In the past decades, the generation and characterization of a large number of mutants have provided unique tools for extensive genetic analysis. Indeed, *C. elegans* has been widely used as a model organism for studying neural development. Despite its small size, an adult hermaphrodite has a nervous system comprising 302 neurons that control a large series of complex behavioral repertoires.[11] Each neuron is classified into a group according to anatomical and functional criteria, while neural circuits have been characterized through the use of genetic mutants, electron micrographs and single-cell imaging of genetically encoded fluorescent proteins. The majority of *C. elegans* neurons are unipolar or bipolar cells with chemically or electrically defined synapses. However, the two sensory PVD neurons in the body and the two FLP neurons in the head of the animal display highly branched dendrites.[12] Given their similarity with mammalian neurons and the suitability of nematodes for genetic analysis, these two classes of neurons have been extensively studied to unveil evolutionarily conserved signaling pathways involved in cell fate specification and morphogenesis.

Here, we investigated dendritic branching in animal models of OXPHOS impairment. In nematodes carrying mutations of complex I/NADH-ubiquinone oxidoreductase subunits, we unexpectedly observed an increased number of dendrites in PVD somatosensory neurons. The same changes were also recapitulated in other sensory neurons in *C. elegans*. We studied the signaling pathways underlying these changes. On the basis of genetic and pharmacological evidence, compromised OXPHOS led to AMPK activation, with PI3K as one of the downstream targets. Taken together, we propose the AMPK/PI3K axis as a critical regulator of dendritic remodeling in conditions of compromised mitochondrial function.

Results

Complex I impairment alters dendritic structures in *C. elegans* sensory neurons. PVD somatosensory neurons are postembryonically generated during the L2 larval stage. The cell soma is positioned in the posterior part of the organism body, while a single axonal projection grows anteriorly and joins the ventral nerve cord. Between the second and third larval stages, PVD neurons extend longitudinally primary branches both in the posterior and anterior part of the body (Figure 1a). At adulthood, PVD neurons display secondary (2°), tertiary (3°) and quaternary (4°) side dendritic branches that envelop the animal body in a dense network of processes underneath the skin.[12,13] Notably, the 2°-3°-4° branches compose elaborate candelabra-like structural units called 'menorahs' (Figure 1b). To visualize PVD menorahs at high-resolution confocal microscopy, we used a *C. elegans* strain expressing the reporter *ser-2prom3::gfp*[14] (Figures 1a and b). Normally, each animal exhibits ~38 of these candelabra-shaped structures and the number shows a constant distribution pattern in individual organisms, although over time there is a considerable decline in the maintenance of the well-organized menorah structure (data not shown). To determine whether impaired OXPHOS

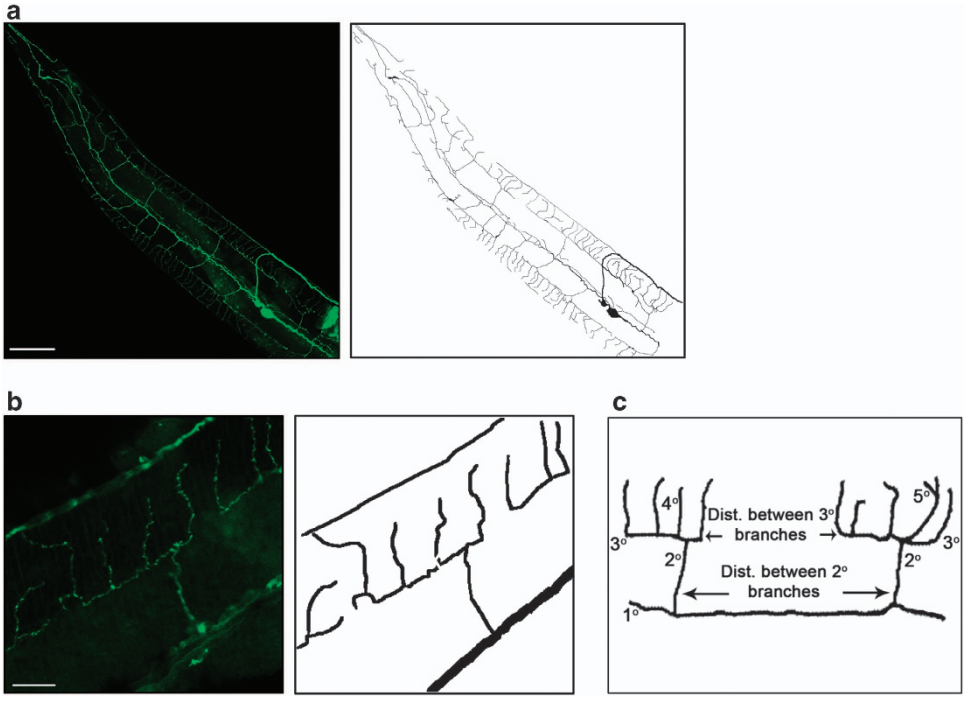

Figure 1 The PVD neuron exhibits an elaborate branching pattern. (**a**) Confocal image (left panel) and schematic tracing (right panel) show a PVD neuron in the posterior part of an animal. Scale bar represents 25 μm. (**b**) Confocal image (left panel) and schematic (right panel) depict at high magnification a representative menorah. Scale bar represents 10 μm. (**c**) Schematic diagram of two menorahs describes the orthogonal dendritic array as organized in 1°, 2°, 3°, 4° and 5° branches and the distance between neighboring 2° and 3° branches, which are measured in this study

can affect dendrites *in vivo*, we simplified our assay by scoring menorahs in the posterior part of the *C. elegans* body on the first day of adulthood. First, we assessed the number of 2° branches per 100 μm. Then, we measured the distance between the 2° and 3° branches, which can be considered the 'stem' and the 'base' of the candelabra-like structure (Figure 1c). In wild-type nematodes, more than 85% of the animals displayed approximately four 2° branches per 100 μm (Figures 2a and b). As a model of severe mitochondrial deficiency, we introduced the integrated *ser-2prom3::gfp* transgene in *gas-1(fc21)* loss-of-function mutant nematodes. The *gas-1(fc21)* is a missense mutation that affects the expression of one subunit of complex I,[15] resulting in impaired mitochondrial respiration and short lifespan. We scored 2° branches in *gas-1* mutants and, interestingly, we observed a significantly increased number of structural units compared with wild-type nematodes (Figures 2a and b). To confirm the increased density of dendritic arbors, we also measured the distance between the 2° and 3° branches. In agreement with our previous observation, we noticed that structural units occurred with an almost double frequency in *gas-1(fc21)* mutant nematodes compared with the wild-type ones (Figures 2c and d). Thus, our *in vivo* analysis suggests that complex I inhibition promotes excessive branching. Furthermore, as the total length of 3° branches was unaffected (Figure 2e), we can conclude that a single menorah covered a significantly smaller receptive field in mitochondrial mutants. To determine whether this phenotype occurs independently of the OXPHOS defect, we analyzed another strain overexpressing *ser-2prom3::gfp* and carrying a missense point mutation in the *nuo-6* gene encoding the NDUFB4/B15 subunit of complex I.[16] In line with our previous evidence in *gas-1* mutants, *nuo-6* mutant nematodes exhibited a significantly increased branching pattern as demonstrated by the number of 2° branches and the decreased distance between them (Figures 2f and g). As animals carrying OXPHOS defects exhibit enhanced oxidative stress,[9,16] we assessed the number of 2° branches in *gas-1* mutants exposed to the antioxidant Vitamin C. Notably, the increased dendritic branching was not affected by antioxidant treatment (Figure 2h). Next, we tested whether compromised OXPHOS affects dendritic architecture in a cell-dependent manner, and, as an additional neuronal cell type, we analyzed the two PLM neurons in a strain overexpressing the integrated *mec-4p::gfp* transgene. The PLM cells are two of the six touch receptor neurons and normally show a single process that anteriorly projects from each soma. Interestingly, whereas in control wild-type animals PLM neurons rarely showed ectopic structures, in *gas-1(fc21)* mutant nematodes there was a twofold increase in extra protrusions (Figures 2i and j). Collectively, our data suggest that impaired mitochondrial ETC causes growth of extra dendritic branches *in vivo* in *C. elegans*, independently of the enhanced oxidative stress and regardless the genetic manipulation.

AMPK activation promotes alteration of dendritic arbors. To determine the mechanisms by which OXPHOS defects induce extra branching in nematodes, we tested potential downstream signaling pathways that might become active due to energy deprivation. Among them, AMPK is a promising candidate as it is a crucial energy sensor involved in many catabolic processes engaged during stress, including conditions of altered mitochondrial respiration. Indeed, decreased energy levels promote the binding of AMP to AMPK, causing an allosteric activation that allows the phosphorylation of Thr172 in the α-kinase domain by upstream kinases like LKB1 or CaMKKβ.[17] In *C. elegans*, both *aak-1* and *aak-2* genes encode two homologs of the α-catalytic subunit of AMPK, with *aak-2* taking part in stress-response signaling pathways due to energy crisis.[18,19] We assessed the phosphorylation status of *C. elegans* AMPK and observed significantly increased levels of phospho-AMPK in homogenates from *gas-1* mutants compared with wild-type animals (Figure 3a). As we did not observe any band in *aak-2*-null mutant nematodes, AAK-2 is likely the main phosphorylated AMPK (Figure 3a). Next, we generated *gas-1; aak-2* double mutant animals overexpressing the fluorescent reporter *ser-2prom3::gfp*. While *gas-1* loss-of-function caused consistent increased dendritic branching, neither the number of menorahs and 2° branches nor the distance between 2° branches was considerably different in *gas-1; aak-2* double mutants compared with wild-type nematodes (Figures 3b–d). This suggests that AAK-2/AMPK is required to promote extra branching as a result of OXPHOS deficiency. In mammals, during neuronal polarization AMPK overactivation disrupts the PI3K association with kinesin Kif5 and the consequent axonal transport. Consequently, PI3K is not correctly targeted to the axonal ending and cannot sustain the proper activity of the downstream target Akt.[20] Similarly, PI3K is responsible for netrin-dependent axonal outgrowth during nematode development.[21] To define the eventual role of PI3K in dendrite outgrowth, we generated *C. elegans* strains carrying a loss-of-function allele for the *age-1* gene, which encodes the p110 subunit of PI3K.[22] Consistently with previous studies, *age-1* loss-of-function completely suppressed the increased dendritic branches induced by OXPHOS impairment (Figures 3b–d), supporting the hypothesis that AGE-1/PI3K takes part in the process. We hypothesized that AAK-2/AMPK overactivation would mimic the condition of OXPHOS impairment and lead to a comparable enhancement of dendritic branching. Thus, we exposed nematodes to the 5-amino-imidazole-carboxamide riboside (AICAR), an AMP mimetic that directly activates AMPK and was previously suggested as a therapeutic approach in the treatment of mitochondrial disorders.[23] In line with our hypothesis, AICAR stimulated AAK-2/AMPK (Figure 3e) and promoted dendritic branching in wild-type nematodes, but it did not further increase the menorah number in *gas-1(fc21)* animals, suggesting that the AAK-2/AMPK pathway is already engaged during OXPHOS impairment (Figure 3f). At the protein level, the decreased P-AMPK in *aak-2*-null mutants confirmed the specificity of AICAR (Figure 3e). Notably, AICAR did not promote dendritic branching in *aak-2* mutant animals (Figure 3g). Finally, to determine whether AAK-2 acts upstream AGE-1, we hypothesized that AICAR treatment would not promote extra branching in *age-1* mutants. In support of this view, we found that *age-1* loss-of-function considerably suppressed the effect of AICAR (Figure 3h). This strongly suggests that AAK-2/AMPK induces dendritic branching through AGE-1/PI3K.

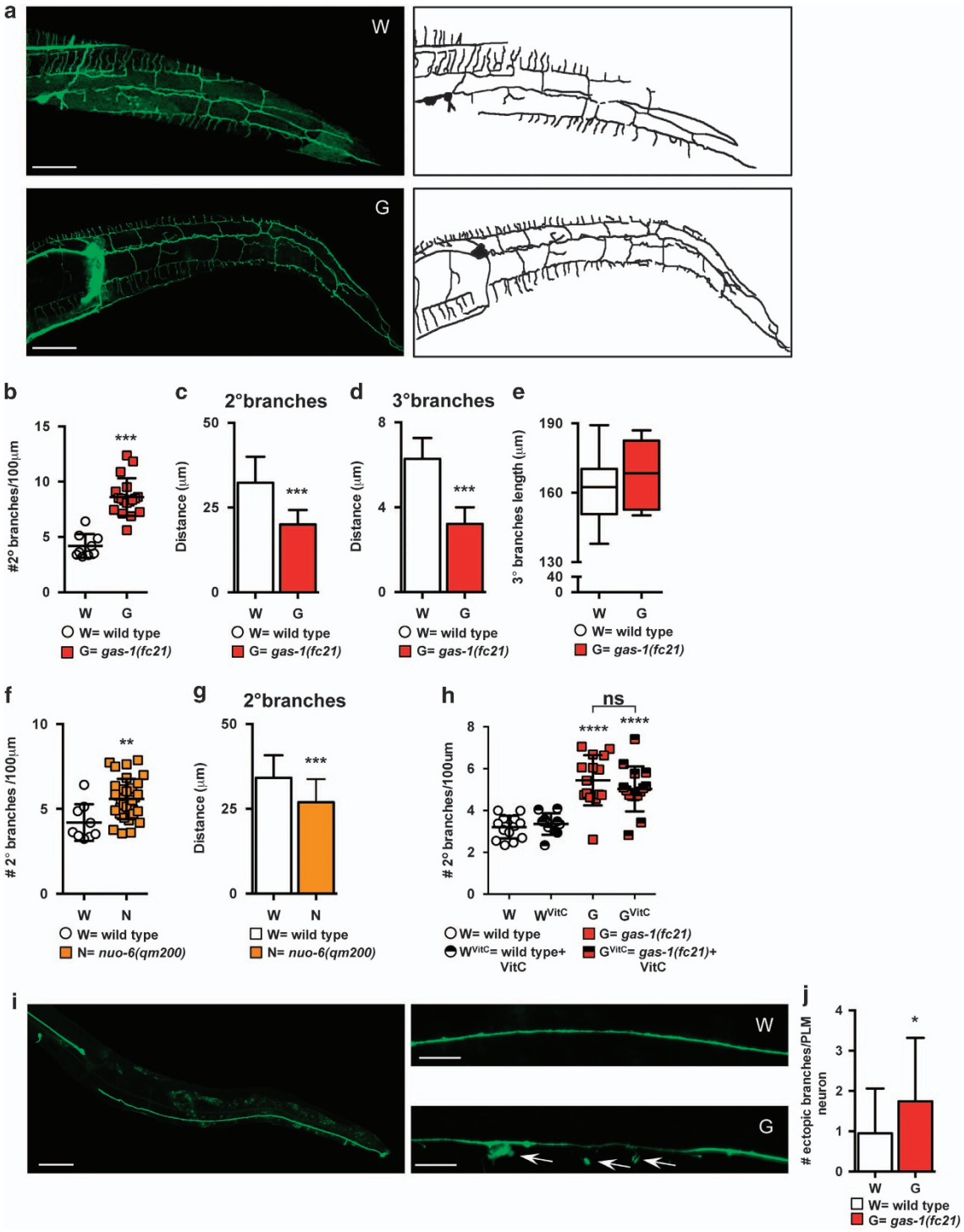

Figure 2 Mitochondrial complex I deficiency increases the branching of *C. elegans* neurons. (**a**) Confocal images (left panel) and schematic traces (right panel) of wild-type (W) and *gas-1(fc21)* (G) mutant nematodes overexpressing the *ser-2prom3::gfp* transgene. Scale bars represent 25 μm. (**b**) Quantification of 2° branches in wild-type and *gas-1* mutant nematodes. (**c**,**d**) Distance between 2° (**c**) and 3° (**d**) branches in wild-type and *gas-1* mutant nematodes. (**e**) Quantification of the length of the 3° branches in wild-type and *gas-1* mutant nematodes. (**f**,**g**) Quantification of 2° branches normalized to the body length (**f**) and the distance between 2° branches (**g**) in wild-type and *nuo-6* mutant nematodes. (**h**) Quantification of 2° branches normalized to the body length for wild-type and *gas-1* mutant nematodes after treatment with 1 mM Vitamin C. (**i**) Representative confocal image of a wild-type animal (left panel) overexpressing the *mec-4p::gfp* transgene. Scale bar represents 50 μm. Representative confocal images (right panel) of a part of the PLM neuron of a wild-type (W) and a *gas-1* mutant nematode (G) overexpressing the *mec-4p::gfp* transgene. The arrows indicate the ectopic processes. Scale bars represent 10 μm. (**j**) Quantification of ectopic processes in PLM neurons in wild-type (W) and *gas-1* (G) mutants. ****$P<0.0001$, ***$P=0.0001$, **$P<0.001$, *$P<0.05$, one-way ANOVA (panel H) or Student's *t*-test; $n=3$ for each set of experiment

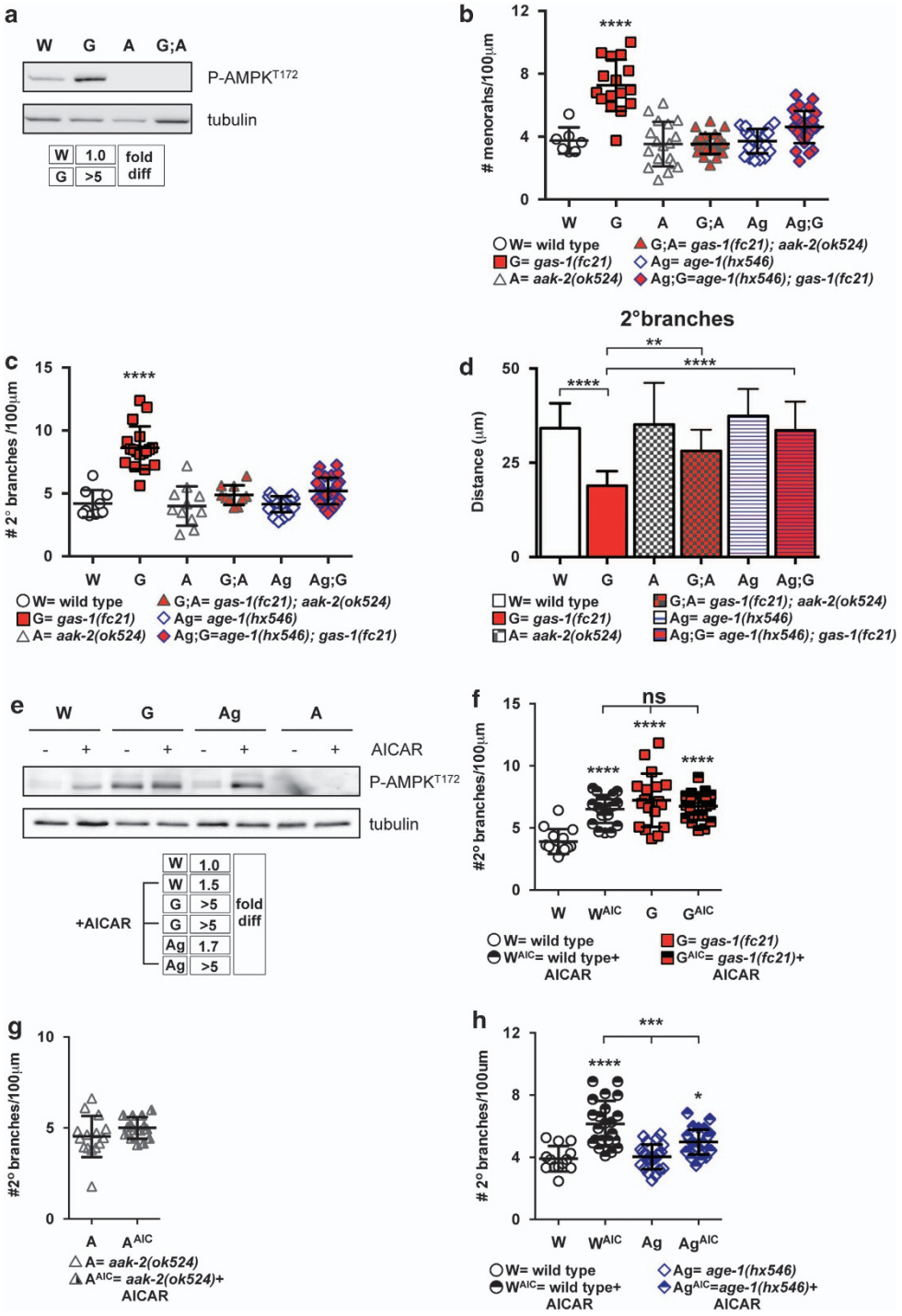

Figure 3 AMPK controls dendritic branching in nematodes with compromised OXPHOS. (**a**) Immunoblot analysis of phosphorylated AMPK (T172) and tubulin (loading control) in protein extracts from wild-type (W), *gas-1* (G), *aak-2* (A) and *gas-1; aak-2* (G;A) mutant nematodes ($n = 1$). (**b**,**c**) Quantification of menorah number (**b**), number of 2° branches (**c**) and distance between 2° branches (**d**) in wild-type, *gas-1*, *aak-2*, *gas-1; aak-2*, *age-1* and *age-1; gas-1* mutant nematodes. The number of menorahs and of 2° branches is normalized to the body length. (**e**) Immunoblot analysis of phosphorylated AMPK (T172) (tubulin as loading control) for untreated and treated with 1 mM AICAR wild-type (W), *gas-1* (G) *age-1* (Ag) and *aak-2* (A) mutant nematodes ($n = 1$). (**f**) Number of 2° branches normalized to the body length in wild type and *gas-1* mutant animals untreated or treated with 1 mM AICAR. (**g**) Number of normalized 2° branches in *aak-2* mutant animals exposed to 1 mM AICAR. (**h**) Number of 2° branches normalized to the body length in wild-type and *age-1* mutant animals untreated or treated with 1 mM AICAR. ****$P < 0.0001$, ***$P < 0.001$, **$P < 0.01$, *$P < 0.05$, one-way ANOVA, $n = 3$ (unless otherwise indicated) for each set of experiments and 15–30 animals per condition were analyzed in total

OXPHOS impairment-induced dendritic branching is uncoupled from accelerated aging. Lastly, to rule out that the observed phenotype was simply due to premature aging, we assessed the morphology of PVD neurons in *daf-2* mutant animals. Inhibition of the sole insulin/IGF-1 receptor results in enhanced cellular maintenance and prolonged lifespan.[24]

Moreover, reduced insulin/IGF-1 signaling suppresses neurite branching.[25,26] We generated animals overexpressing the *ser-2prom3::gfp* transgene, carrying the *gas-1(fc21)* mutation and the hypomorphic allele *daf-2(e1370)*. We observed that the phosphorylation status of *C. elegans* AMPK was significantly higher in the *daf-2* background compared with wild type (Figure 4a). Then, we assessed dendrites in *daf-2* mutants. Although *daf-2; gas-1* double mutants live much longer than *daf-2* single mutant and almost three times longer than *gas-1(fc21)* animals (Troulinaki *et al*, manuscript in preparation), they displayed the same increased number of 2° branches accompanied by reduced distance between branches as in *gas-1* and *daf-2* single mutant nematodes (Figures 4b and c). This is in line with our previous data in the long-lived *nuo-6* mutant nematodes (Figures 2f and g). Overall, our findings suggest that defective OXPHOS leads to dendritic branching through the modulation of the AMPK/PI3K signaling pathway (Figure 4d). Moreover, they rule out that the increased number of structural units in animals with compromised OXPHOS is the result of premature aging.

Discussion

Cognitive decline is a common feature of many neurodegenerative disorders and is associated with the loss of neuronal connectivity. In inherited and sporadic cases of human brain pathologies, a persistent age-related impairment of synaptic structures inevitably affects the spatial and temporal neurotransmission between cells, severely compromises the dynamic remodeling of neural circuits and ultimately results in human intellectual disabilities. In this regard, mitochondrial function significantly contributes to the maintenance of both pre- and postsynaptic compartments, thus affecting existing synapses as well as the formation of new ones.[27,28] Here, we uncover a new signaling cascade that participates in dendritic remodeling as a result of mitochondrial impairment. In animals carrying OXPHOS defects, we provide multiple lines of evidence that illustrate the engagement of the AMPK/PI3K axis and the consequent development of newly formed dendritic branches. Several clues strongly suggest that defined signaling cascades regulate neuronal branching *in vivo*. For example, the serine threonine kinase LKB1 controls axon specification and branching through the activation of the AMPK-like kinase NUAK1 and the consequent stalling of mitochondria at the nascent presynaptic compartment.[29] Similarly, AICAR-mediated AMPK activation affects PI3K localization and Akt activity at the neurite tips during development. This initiates a rapid cascade of detrimental signals that inevitably suppresses axonal growth and neuronal polarization.[20] In our settings, we demonstrated that, in animals carrying mitochondrial defects, OXPHOS inhibition promotes AMPK activity, which then affects the PI3K signaling pathway and the maintenance of the correct dendritic structure.

Beside their role in ATP production, mitochondria are essential in shaping intracellular signaling, especially calcium and cyclic AMP homeostasis.[30,31] In neurons, intracellular distribution of mitochondria can stimulate the formation of synapses. Although mitochondria are rarely observed within dendritic protrusions, their number critically influences the density, plasticity and turnover of spines.[28] In response to depolarizing stimuli, mitochondria tend to concentrate particularly in the vicinity of subcellular compartments characterized by high neuronal activity. Most likely, local recruitment of mitochondria underneath the postsynaptic terminus or at the growth cone might provide metabolic support or high

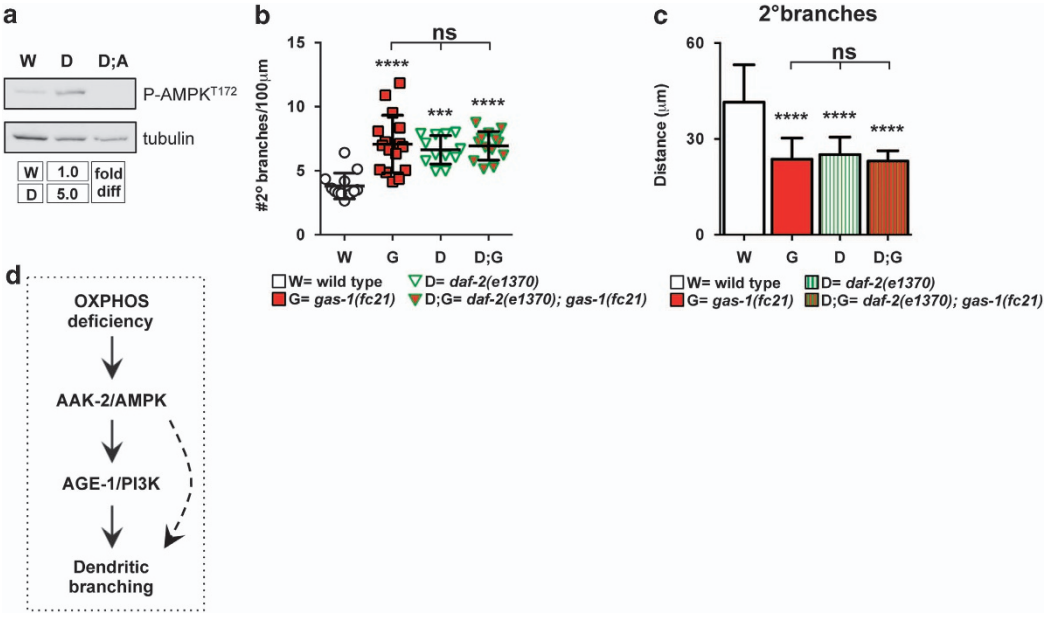

Figure 4 Inhibition of the DAF-2/insulin/IGF-1 signaling pathways does not repress OXPHOS impairment-induced branching. (**a**) Immunoblot analysis of phosphorylated AMPK (T172) and tubulin in samples from wild-type (W), *daf-2* (D) and *daf-2; aak-2* (D;A) mutant nematodes ($n=1$). (**b**,**c**) Measurement of the number of 2° branches normalized to the body length (**b**) and the distance between 2° branches (**c**) in wild-type, *gas-1*, *daf-2* and *daf-2; gas-1* mutant nematodes (****$P<0.0001$, ***$P<0.001$, ns = not significant, one-way ANOVA, $n=3$ and 15–20 animals per condition were analyzed in total). (**d**) Schematic summary of the proposed signaling cascade

calcium buffer capacity. Additionally, in the presence of proper stimulating factors, PI3K-mediated recruitment of mitochondria can stimulate local protein synthesis and, at least in axons, promote branching.[32,33] Thus, in animals with mitochondrial impairment, it would not be surprising that, through AAK-2/AMPK and AGE-1/PI3K, changes in mitochondrial numbers or dynamics potentiate dendritic branching. This would be in line with the observation that mitochondria often localize at the branching sites of new dendritic projections.[26]

Previously published works demonstrated that aging severely affects the maintenance of neuronal structures.[25,26] In agreement with these findings, we confirm that over time PVD neurons exhibit an age-dependent decline of their well-defined spatial organization (data not shown). However, changes in dendritic arbors caused by OXPHOS impairment are not the result of premature aging, as supported by our data in the long-lived *daf-2* and *nuo-6* mutant animals. It is intriguing and perhaps counterintuitive that, in impaired energy conditions, *C. elegans* neurons enhance rather than suppress branching. Perhaps sustained activation of essential cellular sensors causes the loss of a well-organized neuronal architecture by inducing the formation of newly generated branches. Alternatively, additional structural components might be a compensatory event due to decreased functionality. Our findings clearly demonstrate a signaling pathway that controls dendritic branching through AMPK/PI3K under conditions of mitochondrial OXPHOS impairment. Previous studies have described the involvement of AMPK, PI3K and mitochondria in axon guidance and growth.[20,21,32] It is very well possible that the signaling pathway described here might be of relevance also for the remodeling of presynaptic structures and axonal branching under conditions of impaired OXPHOS. Future investigations will be necessary to have a more comprehensive understanding of this important aspect, which is relevant in neurodegenerative disorders associated with mitochondrial deficiency.

Materials and Methods

Antibodies and reagents. The following antibodies and reagents were used in this study: anti P-AMPK (T172) (Cell Signaling, Danvers, MA, USA), anti-tubulin (SIGMA, St. Louis, MO, USA), HRP-conjugated anti-rabbit and anti-mouse secondary antibodies (Thermo Fisher Scientific, Waltham, MA, USA), AICAR (Toronto Research Chemicals Inc., Toronto, ON, Canada) and Vitamin C (SIGMA).

***C. elegans* maintenance and strains.** Nematodes were maintained according to standard procedures.[34] AICAR and Vitamin C were added directly to the nematode growth medium at a final concentration of 1 mM. Then, plates were seeded with *Escherichia coli* OP50 and animals were exposed to the treatment from hatching until the first day of adulthood. The strains used in this study were the following: OH1422 *otls138* [*ser-2*prom3::*gfp*; *rol-6*], SK4005 *zdls5* [*mec-4p::gfp*; *lin-15*(+) (pSK1)], *nuo-6(qm200)I*; *otls138* [*ser-2*prom3::*gfp*; *rol-6*], BAN54 *gas-1*(*fc21*)*X*; *otls138* [*ser-2*prom3::*gfp*; *rol-6*], BAN73 *daf-2(e1370)III; otls138* [*ser-2*prom3::*gfp*; *rol-6*], BAN74 *aak-2*(*ok524*)*X*; *otls138* [*ser-2*prom3::*gfp*; *rol-6*], BAN75 *daf-2(e1370)III; gas-1*(*fc21*)*X*; *otls138* [*ser-2*prom3::*gfp*; *rol-6*], BAN83 *gas-1*(*fc21*)*X*; *aak-2*(*ok524*)*X*; *otls138* [*ser-2*prom3::*gfp*; *rol-6*], BAN102 *gas-1*(*fc21*)*X*; *zdls5* [*mec-4::gfp*; *lin-15*(+) (pSK1)], BAN105 *age-1(hx546)II*; *otls138* [*ser-2*prom3::*gfp*; *rol-6*], BAN117 *age-1(hx546)II*; *gas-1*(*fc21*)*X*; *otls138* [*ser-2*prom3::*gfp*; *rol-6*].

Confocal microscopy. Nematodes were synchronized and regularly transferred on freshly seeded plates with *E. coli* OP50 bacteria. At the first day of adulthood, they were mounted on a drop of mounting medium (30% PEG 8000 in 25% glycerol), covered with a coverslip and imaged using on a Zeiss LSM700 confocal microscope with a $\times$ 40 objective (Carl Zeiss Foundation, Jena, Germany). Quantitative analysis of sequential images was performed with ZEN software (Carl Zeiss Foundation).

Statistical analysis. Statistical analysis was performed using GraphPad Prism software (Graphpad Software, Inc., La Jolla, CA, USA) and the appropriate statistical test was applied as described. For each group, 15–30 animals were analyzed. Data are mean ± S.E.M.

Conflict of Interest

The authors declare no conflict of interest.

Acknowledgements. We thank Ms Christiane Bartling-Kirsch, Ms Gabriele Fleger and Dr. Miriam Jakubik for their technical support. We acknowledge Prof. Sigfriend Hekimi for providing a strain used in this work. We thank many colleagues for their constructive comments. Some strains were provided by the CGC, which is funded by NIH Office of Research Infrastructure Programs (P40 OD010440). Part of the funding for this research was provided by the (DZNE, CIHR, MRC), through the CoEN initiative (www.coen.org).

1. Wallace DC, Fan W, Procaccio V. Mitochondrial energetics and therapeutics. *Annu Rev Pathol* 2010; **5**: 297–348.
2. Koopman WJ, Distelmaier F, Smeitink JA, Willems PH. OXPHOS mutations and neurodegeneration. *EMBO J* 2012; **32**: 9–29.
3. Schagger H, Pfeiffer K. Supercomplexes in the respiratory chains of yeast and mammalian mitochondria. *EMBO J* 2000; **19**: 1777–1783.
4. Lapuente-Brun E, Moreno-Loshuertos R, Acin-Perez R, Latorre-Pellicer A, Colas C, Balsa E *et al.* Supercomplex assembly determines electron flux in the mitochondrial electron transport chain. *Science* 2013; **340**: 1567–1570.
5. Vafai SB, Mootha VK. Mitochondrial disorders as windows into an ancient organelle. *Nature* 2012; **491**: 374–383.
6. Koopman WJ, Willems PH, Smeitink JA. Monogenic mitochondrial disorders. *N Engl J Med* 2012; **366**: 1132–1141.
7. Zeviani M, Di Donato S. Mitochondrial disorders. *Brain* 2004; **127**: 2153–2172.
8. Troulinaki K, Bano D. Mitochondrial deficiency: a double-edged sword for aging and neurodegeneration. *Front Genet* 2012; **3**: 244.
9. Hekimi S, Lapointe J, Wen Y. Taking a "good" look at free radicals in the aging process. *Trends Cell Biol* 2011; **21**: 569–576.
10. Schon EA, Przedborski S. Mitochondria: the next (neurode)generation. *Neuron* 2011; **70**: 1033–1053.
11. de Bono M, Maricq AV. Neuronal substrates of complex behaviors in *C. elegans*. *Annu Rev Neurosci* 2005; **28**: 451–501.
12. Smith CJ, Watson JD, Spencer WC, O'Brien T, Cha B, Albeg A *et al.* Time-lapse imaging and cell-specific expression profiling reveal dynamic branching and molecular determinants of a multi-dendritic nociceptor in *C. elegans*. *Dev Biol* 2010; **345**: 18–33.
13. White JG, Southgate E, Thomson JN, Brenner S. The structure of the nervous system of the nematode *Caenorhabditis elegans*. *Philos Trans R Soc Lond B, Biol Sci* 1986; **314**: 1–340.
14. Tsalik EL, Niacaris T, Wenick AS, Pau K, Avery L, Hobert O. LIM homeobox gene-dependent expression of biogenic amine receptors in restricted regions of the *C. elegans* nervous system. *Develop Biol* 2003; **263**: 81–102.
15. Kayser EB, Morgan PG, Hoppel CL, Sedensky MM. Mitochondrial expression and function of GAS-1 in Caenorhabditis elegans. *J Biol Chem* 2001; **276**: 20551–20558.
16. Yang W, Hekimi S. Two modes of mitochondrial dysfunction lead independently to lifespan extension in *Caenorhabditis elegans*. *Aging Cell* 2010; **9**: 433–447.
17. Hardie DG. AMP-activated protein kinase: an energy sensor that regulates all aspects of cell function. *Genes Dev* 2011; **25**: 1895–1908.
18. Apfeld J, O'Connor G, McDonagh T, DiStefano PS, Curtis R. The AMP-activated protein kinase AAK-2 links energy levels and insulin-like signals to lifespan in *C. elegans*. *Genes Dev* 2004; **18**: 3004–3009.
19. Curtis R, O'Connor G, DiStefano PS. Aging networks in *Caenorhabditis elegans*: AMP-activated protein kinase (aak-2) links multiple aging and metabolism pathways. *Aging Cell* 2006; **5**: 119–126.
20. Amato S, Liu X, Zheng B, Cantley L, Rakic P, Man HY. AMP-activated protein kinase regulates neuronal polarization by interfering with PI 3-kinase localization. *Science* 2011; **332**: 247–251.
21. Chang C, Adler CE, Krause M, Clark SG, Gertler FB, Tessier-Lavigne M *et al.* MIG-10/lamellipodin and AGE-1/PI3K promote axon guidance and outgrowth in response to slit and netrin. *Curr Biol* 2006; **16**: 854–862.
22. Friedman DB, Johnson TE. A mutation in the age-1 gene in *Caenorhabditis elegans* lengthens life and reduces hermaphrodite fertility. *Genetics* 1988; **118**: 75–86.
23. Viscomi C, Bottani E, Civiletto G, Cerutti R, Moggio M, Fagiolari G *et al.* In vivo correction of COX deficiency by activation of the AMPK/PGC-1alpha axis. *Cell Metab* 2011; **14**: 80–90.

24. Kenyon C, Chang J, Gensch E, Rudner A, Tabtiang R. A *C. elegans* mutant that lives twice as long as wild type. *Nature* 1993; **366**: 461–464.
25. Tank EM, Rodgers KE, Kenyon C. Spontaneous age-related neurite branching in *Caenorhabditis elegans*. *J Neurosci* 2011; **31**: 9279–9288.
26. Toth ML, Melentijevic I, Shah L, Bhatia A, Lu K, Talwar A *et al.* Neurite sprouting and synapse deterioration in the aging *Caenorhabditis elegans* nervous system. *J Neurosci* 2012; **32**: 8778–8790.
27. Cheng A, Hou Y, Mattson MP. Mitochondria and neuroplasticity. *ASN Neuro* 2010; **2**: e00045.
28. Li Z, Okamoto K, Hayashi Y, Sheng M. The importance of dendritic mitochondria in the morphogenesis and plasticity of spines and synapses. *Cell* 2004; **119**: 873–887.
29. Courchet J, Lewis TL Jr., Lee S, Courchet V, Liou DY, Aizawa S *et al.* Terminal axon branching is regulated by the LKB1-NUAK1 kinase pathway via presynaptic mitochondrial capture. *Cell* 2013; **153**: 1510–1525.
30. Rizzuto R, De Stefani D, Raffaello A, Mammucari C. Mitochondria as sensors and regulators of calcium signalling. *Nat Rev Mol Cell Biol* 2012; **13**: 566–578.
31. Di Benedetto G, Scalzotto E, Mongillo M, Pozzan T. Mitochondrial Ca(2)(+) uptake induces cyclic AMP generation in the matrix and modulates organelle ATP levels. *Cell Metab* 2013; **17**: 965–975.
32. Spillane M, Ketschek A, Merianda TT, Twiss JL, Gallo G. Mitochondria coordinate sites of axon branching through localized intra-axonal protein synthesis. *Cell Rep* 2013; **5**: 1564–1575.
33. Chada SR, Hollenbeck PJ. Mitochondrial movement and positioning in axons: the role of growth factor signaling. *J Exp Biol* 2003; **206**: 1985–1992.
34. Brenner S. The genetics of *Caenorhabditis elegans*. *Genetics* 1974; **77**: 71–94.